

Date of publication xxxx 00, 0000, date of current version xxxx 00, 0000.

Digital Object Identifier 10.1109/ACCESS.2017.Doi Number

# Metamaterial-Inspired Antenna Array for Application in Microwave Breast Imaging Systems for Tumor Detection

Mohammad Alibakhshikenari<sup>1</sup>, Member, IEEE, Bal S. Virdee<sup>2</sup>, Senior Member, IEEE, Pancham Shukla<sup>2</sup>, Member, IEEE, Naser Ojaroudi Parchin<sup>3</sup>, Member, IEEE, Leyre Azpilicueta<sup>4</sup>, Senior Member IEEE, Chan H. See<sup>5</sup>, Senior Member, IEEE, Raed A. Abd-Alhameed<sup>3</sup>, Senior Member, IEEE, Francisco Falcone<sup>6,7</sup>, Senior Member, IEEE, Isabelle Huynen<sup>8</sup>, Senior Member IEEE, Tayeb A. Denidni<sup>9</sup>, Fellow IEEE, and Ernesto Limiti<sup>1</sup>, Senior Member, IEEE

<sup>1</sup>Electronic Engineering Department, University of Rome "Tor Vergata", Via del Politecnico 1, 00133, Rome, Italy

<sup>2</sup>London Metropolitan University, Center for Communications Technology, London N7 8DB, UK

<sup>3</sup>Faculty of Engineering & Informatics, University of Bradford, Bradford, West Yorkshire, BD7 1DP, UK

<sup>4</sup>School of Engineering and Sciences, Tecnológico de Monterrey, NL 64849, Mexico

<sup>5</sup>School of Eng. & the Built Environment, Edinburgh Napier University, 10 Colinton Rd., Edinburgh, EH10 5DT, UK

<sup>6</sup>Electric, Electronic and Communication Engineering Department, Public University of Navarre, 31006 Pamplona, Spain

<sup>7</sup>Institute of Smart Cities, Public University of Navarre, 31006 Pamplona, Spain

<sup>8</sup>Institute of Information and Communication Technologies, Electronics and Applied Mathematics, Université Catholique de Louvain, Belgium

<sup>9</sup>Institut National de la Recherche Scientifique (INRS), University of Quebec, Montreal, QC, Canada

Corresponding author: M. Alibakhshikenari (e-mail: alibakhshikenari@ing.uniroma2.it)

**ABSTRACT** This paper presents a study of a planar antenna-array inspired by the metamaterial concept where the resonant elements have sub-wavelength dimensions for application in microwave medical imaging systems for detecting tumors in biological tissues. The proposed antenna consists of square-shaped concentric-rings which are connected to a central patch through a common feedline. The array structure comprises several antennas that are arranged to surround the sample breast model. One antenna at a time in the array is used in transmission-mode while others are in receive-mode. The antenna array operates over 2-12 GHz amply covering the frequency range of existing microwave imaging systems. Measured results show that compared to a standard patch antenna array the proposed array with identical dimensions exhibits an average radiation gain and efficiency improvement of 4.8 dBi and 18%, respectively. The average reflection-coefficient of the array over its operating range is better than  $S_{11} \leq -20$  dB making it highly receptive to weak signals and minimizing the distortion encountered with the transmission of short duration pulse-trains. Moreover, the proposed antenna-array exhibits high-isolation on average of 30dB between radiators. This means that antennas in the array (i) can be closely spaced to accommodate more radiators to achieve higher-resolution imaging scans, and (ii) the imagining scans can be done over a wider frequency range to ascertain better contrast in electrical parameters between malignant tumor-tissue and the surrounding normal breast-tissue to facilitate the detection of breast-tumor. It is found that short wavelength gives better resolution. In this experimental study a standard biomedical breast model that mimics a real-human breast in terms of dielectric and optical properties was used to demonstrate the viability of the proposed antenna over a standard patch antenna in the detection and the localization of tumor. These results are encouraging for clinical trials and further refinement of the antenna-array.

**INDEX TERMS** Array antenna; microstrip technology; metamaterial; microwave breast imaging systems; biosensor, tumor detection; cancer; medical imaging

## I. INTRODUCTION

Medical imaging is an effective technique in diagnosing and treating a variety of diseases by providing a visual

representation of inner organs of the human body [1,2]. Surgical intervention can be avoided by using such diagnostic imaging systems. Also, such imaging modalities

have become vital in monitoring the effectiveness of treatment for diagnosed tumor [3] and to promote public health for all population groups and at all levels of health care [4,5]. Various medical imaging technologies have been developed over the past few decades including ultrasound, computed tomography (CT), magnetic resonance imaging (MRI) and nuclear medicine imaging. However, despite of their great advantage in terms of image resolution and accuracy, medical imaging technologies other than ultrasound are highly expensive pieces of equipment which are rarely available at rural and remote health centers. According to the World Health Organization (WHO), more than half of the world's population does not have access to diagnostic imaging [6]. Consequently, there is a high demand on a low-cost, reliable, and safe imaging system for detecting and monitoring cancer.

Existing imaging systems based on ionization radiation have a limited permissible exposure dosage and cannot be used frequently on pregnant women and children. In recent years, much effort has been devoted to find a reliable cancer diagnostic tool using non-ionization radiation. Techniques based on electromagnetic (EM) energy in the microwave region have been investigated for image reconstruction [7,8]. Compared to existing imaging systems, microwave imaging can be safely repeated more frequently because it is free from ionizing radiation [9-11]. In fact, investigations show that microwaves allow dielectric properties of healthy and malignant tissues to be contrasted which enables medical images to be created relatively easily due to the interaction of EM waves with matter [12]. This is because interaction of EM waves and matter is a function of dielectric properties which can be directly related to various types of biological constituents due to their varying degree of water content: bone, fat, muscle, etc. [13].

It can be concluded from previous studies that an excellent compromise can be reached between image resolution and signal penetration into biological tissues with the use of either a single high directivity ultra-wideband (UWB) antenna or an antenna array [14]. In the frequency range between 1 GHz to 10 GHz, the EM waves penetrate biological tissue very effectively and with acceptable attenuation [8], however, at higher frequencies greater than 10 GHz the EM waves are scattered on the skin surface [15].

Detection of cancer can be achieved by electrically characterizing the biological tissue under investigation. This is usually done using highly directive microwave antennas in the microwave imaging system. The antennas are used to detect the changes in the permittivity of the biological tissue. Permittivity is normally high at lower frequencies due to an insulating effect of cell membranes and reduces at higher frequencies due to scattering effects [13]. Antennas pose one of the key challenges in imaging systems as the physical size of antenna is a function of

wavelength at the operating frequency. A reduction in antenna size is essential to enable a greater number of antennas to be incorporated inside the imaging system so that more information can be gathered from the scattered signals for high resolution image reconstruction. In addition, the antenna needs to have a wide impedance bandwidth to obtain high-resolution images and minimize the distortion encountered with the transmission of short duration pulse trains [16]. Several antennas have already been proposed for cancer detection including monopole antennas [17], fractal antennas [18], antipodal Vivaldi antennas [19], slot antenna [20], and patch antenna [21].

In this paper, we have demonstrated that the proposed metamaterial inspired antenna exhibits a very large impedance bandwidth for  $S_{11} \leq -20$  dB without increasing its physical footprint. The proposed antenna is intended for use in a biosensor array to detect malignant tumors in breasts. Its wide impedance bandwidth means that scans can be done over a larger frequency spectrum to provide significantly better contrast in the images between the tumor tissue and the surrounding breast-tissue. The results presented show that proposed antenna offers a higher gain and radiation efficiency performance than an equivalent standard patch antenna of identical dimensions. It is also shown that the performance of the proposed antenna array is superior compared to other antenna arrays reported in literature in terms of gain, reflection-coefficient, and impedance bandwidth.

The paper is organized as follows: in section II, the electrical properties of biological tissue are discussed briefly. This section is divided to two sub-sections including: i) dielectric properties of breast tissues, and ii) modelling of biological tissue. In section III, the proposed antenna array is presented. Information on the imaging set-up and measurements is given in section IV. Finally, the paper is concluded in section V.

## II. ELECTRICAL PROPERTIES OF BIOLOGICAL TISSUE

The contrast in dielectric properties of healthy tissues and the malignant tissues can be exploited to detect cancer cells by microwave imaging techniques [22]. This is due to the variation in the water content in tissue cells which results in marked electrical properties [23]. These findings are based on numerous studies carried out on various types of biological tissues including breast [24], liver [25], lymph nodes [26], skin [27], bone [28], and heart [29]. The studies reveal distinct electrical properties exhibited by healthy and malignant tissues which are based on water content [30], necrosis [31], sodium content [32], cell membrane charging [33], and dielectric relaxation time variation [34].

### A. DIELECTRIC PROPERTIES OF BREAST TISSUES

Electrical conductivity and relative permittivity measurements in [34] reveal that the contrast in conductivity

between malignant tissue and healthy breast tissue is 6.4:1, and the contrast in relative permittivity between malignant tissue and healthy breast tissue is 3.8:1. In addition, the contrast in the dielectric properties between malignant and healthy tissues is highest for the mammary gland. These results are based on measurement of various tissues from patients including colon, kidney, liver, breast, muscle, and lung over the frequency range of 0.5 GHz to 0.9 GHz.

Experimental measurements in the study conducted in [35] of muscle and malignant tumors, i.e. high-water content tissue cells, show higher dielectric properties than fat and healthy breast tissues, i.e. low water content tissue cells. The measurements were done over the whole microwave spectrum. Investigated in [36] is the dielectric properties of healthy breast tissue and cancerous tissue over the frequency range of 0.5 GHz to 20 GHz. This study reveals that both the dielectric constant and conductivity reduce with increase in adipose, however the dielectric constant and conductivity increase with increase in glandular and fibro-connective tissues. The relative permittivity and conductivity of healthy and malignant breast tissues in the frequency range up to 3 GHz reported in [37] show distinct contrast in the dielectric properties of malignant tissue and healthy breast tissue, which are 4.7:1 and 5:1, respectively.

It can be concluded from the above studies that the relative permittivity and conductivity of tissues with high water content are approximately identical as muscle at frequencies greater than 1 GHz. In contrast, the relative permittivity and conductivity of malignant cancerous tissues are much higher than muscles at frequencies less than 1 GHz [38].

### B. MODELLING OF BIOLOGICAL TISSUE

Dielectric properties of materials including biological tissues vary with frequency of the signal at which they are measured however this dependency is nonlinear [39]. In fact, microwave signals attenuate with increase in frequency which results in a lower depth of penetration. It is therefore important to select an appropriate microwave frequency range for imaging of breasts. Debye and Cole-Cole models are commonly used to model biological tissues [24]. The Debye model is defined by [40]:

$$\epsilon_r = \epsilon_\infty + \frac{\epsilon_s + \epsilon_\infty}{1 + j\omega\tau} - j \frac{\sigma}{\omega\epsilon_0} \quad (1)$$

Where  $\epsilon_\infty$  represents the permittivity and its value strongly corresponds to the water content of the tissue,  $\epsilon_s$  and  $\tau$  represent the static permittivity and the relaxation time, respectively.

The complex dielectric constant of biological tissues is defined by the Cole-Cole model [41] which is given by:

$$\epsilon^*(\omega) = \epsilon_\infty + \frac{\epsilon_s - \epsilon_\infty}{1 + (j\omega\tau)^{1-\alpha}} \quad (2)$$

where the complex dielectric, static and infinite frequency constants, the angular frequency, and the time constant are represented by  $\epsilon^*$ ,  $\epsilon_s$ ,  $\epsilon_\infty$ ,  $\omega$ , and  $\tau$ , respectively. The exponent parameter  $\alpha$  ( $0 < \alpha < 1$ ) represents different spectral shapes. When  $\alpha = 0$ , the Cole-Cole model becomes the Debye model. When  $\alpha > 0$ , the relaxation time is increased.

The relationship between the dielectric parameters and the moisture content model [23] is defined by the empirical model given by:

$$\epsilon'_r = 1.71 f^{1.3} + \frac{\epsilon_s - 4}{1 + (f/25)^2} \quad (3)$$

$$\sigma = 1.35\sigma_{0.1}f^{0.13} + 0.00222f^2 \left[ \frac{\epsilon_s - 4}{1 + (f/25)^2} \right] \quad (4)$$

where  $f$  is the frequency and  $\sigma_{0.1} = 0.05$ , and  $\epsilon_s = 8.5$  [21].

### III. METAMATERIAL INSPIRED ANTENNA ARRAY FOR BREAST CANCER DETECTION

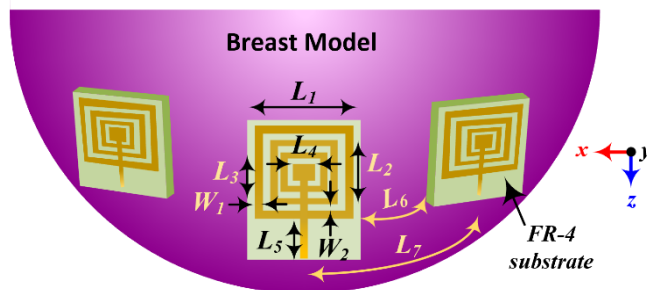
The proposed antenna/sensor array, shown in Fig. 1, consists of several antennas arranged around the breast model. The exact arrangement employed is shown in Fig. 6. The design of the antenna constituting the array is based on a standard square patch. The antenna is composed of several concentric square rings of decreasing size etched on a dielectric substrate and excited from a common feedline. The rings of sub-wavelength dimensions, which is characteristic of metamaterials, act like resonant elements when excited with EM energy [42][43].

The metamaterial inspired antenna array was evaluated using Finite Integration Technique (FIT) based on 3D electromagnetic full-wave CST-Microwave Studio software tool. Dimensions of the ring affect the antenna's performance in terms of impedance bandwidth, radiation patterns, gain, and efficiency. The key parameters of the proposed antenna are: (i) the number of the square rings; (ii) the width of the rings ( $W_1$ ); (iii) the lengths defining the square rings ( $L_1, L_2, L_3, L_4$ ); and (iv) the width of the slots between the rings ( $W_2$ ). The optimized values of the antenna parameters are tabulated in Table. I.

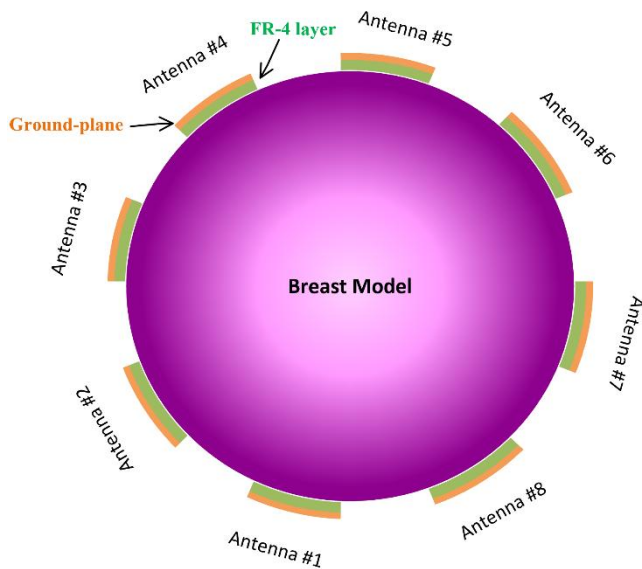
TABLE I  
KEY STRUCTURAL PARAMETERS OF THE PROPOSED ANTENNA AND OVERALL SIZE

Number of rings	3
$L_1$	6.0 mm
$L_2$	4.4 mm
$L_3$	2.8 mm
$L_4$	1.2 mm
$L_5$	2.8 mm
$L_6$	2.8 mm
$L_7$	8.3 mm
$W_1$	0.4 mm
$W_2$	0.4 mm
Array dimensions	$22 \times 22 \times 0.5 \text{ mm}^3$

Each antenna in the array is used transmits microwave pulses in turn while other antennas are configured in receive mode to measure the transmission and reflected signals from abnormalities in the breast. The antennas in the receive mode that are adjacent to the radiating element collect the signals that are reflected off tissue surfaces whereas antennas opposite to the radiating pair collect transmitted signals through the breast tissue. The proposed configuration of sensors enables multi-view of the scattered signal intensity and phase distributions which allow to capture information on the localized dielectric properties of the biological tissue.



(a) Side-view of antenna array arrangement around the breast.



(b) Top-view of antenna array arrangement around the breast.

**FIGURE 1.** Illustration of the proposed antenna array surrounding the breast model.

The proposed antenna array was constructed on FR-4 substrate with a ground-plane on the opposite face. The substrate used had a thickness of 0.5 mm, dielectric constant of 4.3, and loss-tangent of 0.025. The array is configured such that the antennas are strategically located around the breast, as shown in Fig. 1. Proximity of antennas in the arrangement cause unwanted mutual coupling that can adversely affect the antenna's impedance bandwidth,

radiation patterns, gain, and efficiency. However, the effect of mutual coupling is significantly dampened using the proposed antenna in the array as will be shown below in the measured transmission response.

In a typical microwave imaging system such as that described in [17] abnormalities in the breast are identified by applying cost-sensitive ensemble classifiers. Breast scans involve the patient placing their breast in a ceramic hemispherical cup/dome, as illustrated in Fig. 2. Embedded inside the inverted cup are microwave antennas. The antennas in the array, shown in Fig. 1, are driven via a 50  $\Omega$  coaxial feedline where each antenna is connected to a multiplexer whose output is connected to a Vector Network Analyzer to provide the measurements in the time domain. The multiplexer is used to automatically switch one antenna to transmit mode and the others to receive mode. Each antenna in the imaging system transmits microwave pulses in sequence while other antennas are configured to measure the transmission and reflection signals from abnormalities in the breast. This methodology allows precise localization of the tumor. This is the type of imagining modality the proposed antenna is intended for. In such a system each scan typically lasts three minutes and records around 110 signals. The sampling rate of the Vector Network Analyzer we used was 15.625 MHz. The recorded data from the measurements is then evaluated after its been signal processed to remove noise artifacts generated by multiple reflections from the different breast tissue layers.

Characterization of the breast images from the array at microwave frequencies entailed using an inverse scattering technique involving the determination of (i) the incident fields at each antenna in the array from the breast model; (ii) the background dyadic Green's function; and (iii) linking the volume integrals in the imaging algorithms to measurable transmit and receive signals. The measured S-parameters of the scattered fields in the frequency domain were then transformed into the time domain using inverse Fast Fourier Transform (IFFT) for inverse processing.

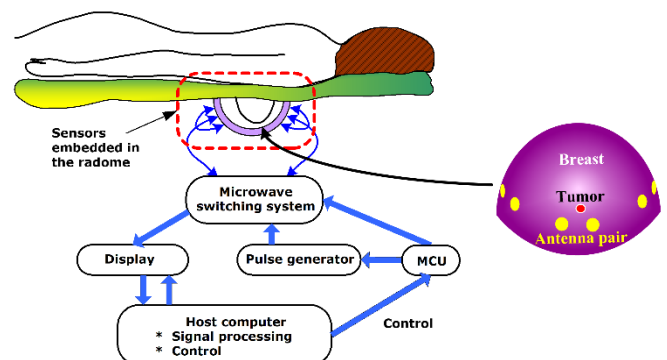
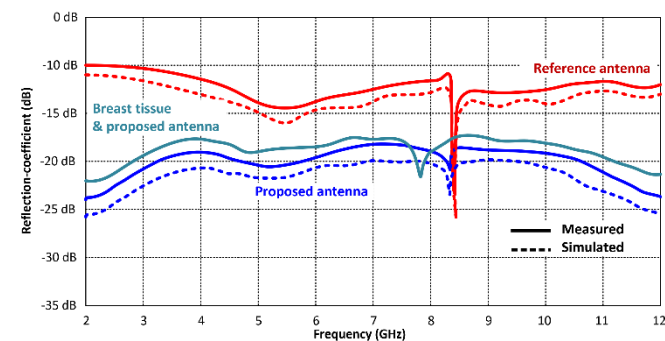
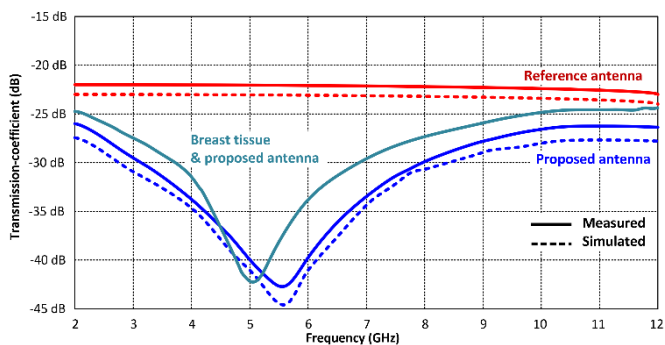


**FIGURE 2.** A typical microwave imaging system in which the proposed antenna array configuration is embedded inside the breast dome.

The measured S-parameters of the proposed antenna array, the proposed antenna array with breast tissue, and a reference antenna array are shown in Fig. 3. The reference antenna array is constructed from equivalent standard square patch antennas. The biomedical phantom breast tissue used in the study had skin thickness of 2 mm and relative permittivity ( $\epsilon$ ) of 36. The relative permittivity of the breast tissue was 10. It is evident from these results that the proposed antenna array provides considerably improved reflection-coefficient over a very large frequency span from 2 GHz to 12 GHz. Over this frequency range the proposed array has an average measured reflection-coefficient better than -20 dB compared to -12 dB by the reference array (standard square patches). The reflection-coefficient of the reference array dips sharply at 8.35 GHz to about -26 dB however although the dip for the proposed array is modest. The magnitude of the dip is about -24 dB. With breast tissue the performance of the proposed array worsens by about 2 dB, which is due to tissue absorption, and its response dips at a slightly lower frequency of 7.8 GHz. Compared to the reference array the proposed array in situ with the breast tissue exhibits an excellent impedance match over a very wide bandwidth (2-12 GHz). This demonstrates it is highly sensitive and receptive to weak signals over this frequency range.



(a) Reflection-coefficient ( $S_{11}$ ) response of reference antenna, proposed antenna, and proposed antenna with breast tissue.

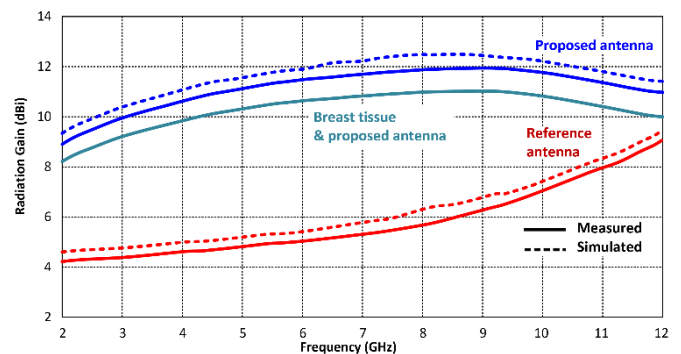


(b) Transmission-coefficient ( $S_{22}$ ) response of reference antenna, proposed antenna, and breast tissue with proposed antenna.

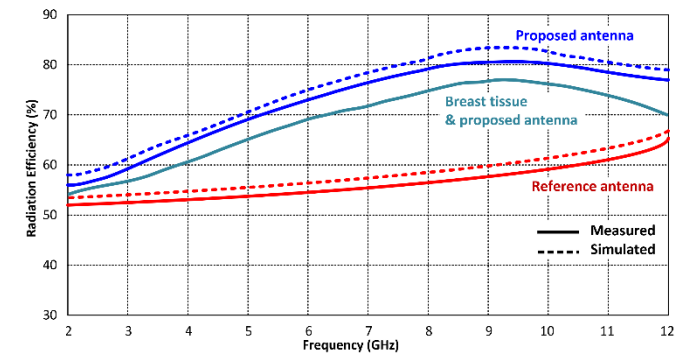
**FIGURE 3.** Measured and simulated S-parameter responses of the antenna array for the reference antenna, the proposed antenna, and the proposed antenna with breast tissue. The reference antenna is an equivalent standard square patch antenna.

Mutual coupling effects between adjacent antennas in an array can adversely affect the arrays radiation characteristics especially when the spacing between the antennas is less than 0.5 wavelength as is the case here and in microwave imaging systems for breast tissue [44, 45]. This is due to the unwanted interactions resulting from surface waves and near-field radiation. This is because patch antennas excite surface waves, which are guided by the substrate and the ground-plane [46-48].

The measured transmission response of the proposed antenna array shows strong suppression of mutual coupling between the adjacent radiating elements by greater than 26 dB across 2 GHz to 12 GHz, and the suppression is strongest, i.e. by 43 dB, at around 5.5 GHz. The isolation is significantly improved because the proposed antenna is constructed from resonators with sub-wavelength dimensions, which is characteristic of metamaterial structures. With breast tissue insertion in the proposed array the suppression is reduced by 1.6-3.8 dB over the antenna's operating range. However, in the case of a reference array the mutual coupling suppression is limited to about -23 dB over 2 GHz to 12 GHz.



(a) Radiation gain response of reference antenna, proposed antenna, and breast tissue with proposed antenna.



(b) Radiation efficiency response of reference antenna, proposed antenna, and breast tissue with proposed antenna.

**FIGURE 4.** Measured and simulated radiation gain and efficiency response of the antenna array for the reference antenna, the proposed antenna, and the proposed antenna with breast tissue. The reference antenna is an equivalent standard square patch antenna.

Comparison of the measured radiation gain and efficiency of the proposed antenna array, proposed antenna array with breast tissue, and the reference array are shown in Fig. 4. The average measured gain and efficiency of the proposed antenna array are 11 dBi and 74%, respectively, across 2 GHz to 12 GHz. With insertion of breast tissue in the proposed array the gain and efficiency of the array worsen on average by about 1 dB and 4%, respectively. Over the same frequency range, the average measured gain and efficiency of the standard square patch antenna array are 6.2 dBi and 56%, respectively. These results clearly demonstrate that compared with a reference array the proposed antenna array offers gain and efficiency improvement by an average of 4.8 dB and 18%. The comparison between the reference array, proposed array, and proposed array with breast tissue is summarized in Table II.

TABLE II  
MEASURED RADIATION CHARACTERISTICS OF ANTENNA ARRAY

Radiation gain	Reference antenna	Proposed antenna	Proposed antenna with breast tissue
Minimum	4.2 dBi @ 2 GHz	8.9 dBi @ 2 GHz	8.1 dBi @ 2 GHz
Maximum	9.1 dBi @ 12 GHz	12 dBi @ 9 GHz	11 dBi @ 9 GHz
Average	6.2 dBi	11 dBi	10 dBi

Radiation efficiency	Reference antenna	Proposed antenna	Proposed antenna with breast tissue
Minimum	52% @ 2 GHz	56% @ 2 GHz	51% @ 2 GHz
Maximum	64% @ 12 GHz	81% @ 9 GHz	74% @ 9 GHz
Average	56%	74%	64%

Table III shows a comparison between the performance parameters of the proposed antenna and other planar antennas recently reported in literature. It is evident that the proposed antenna has a relatively small form factor in comparison to other antennas for microwave breast imaging systems. It is also evident from that the proposed antenna outperforms other antennas in terms of gain, reflection-coefficient, and impedance bandwidth performance.

TABLE III  
PERFORMANCE COMPARISON OF THE PROPOSED ANTENNA WITH OTHER ANTENNAS REPORTED IN LITERATURE

Parameters	This work	[49]	[50]	[51]	[52]	[53]
Antenna dimensions (mm <sup>2</sup> )	22×22	76×78	42×48	25×16	125×51	25×25
Ave. reflection-coefficient (dB)	-20	-15	-8.5	NR	-12	-20
Ave. Gain (dBi)	11	7	6.7	3.5	NR	6.6
Ave. Eff. (%)	74	80	NR	NR	NR	NR
Imp. Bandwidth (GHz) for S <sub>11</sub> ≤ -10dB	10	5	0.9	0.9	0.002	0.26

NR: not reported

## VI. IMAGING SETUP AND MEASUREMENT

The effectiveness of the proposed antenna was tested using a standard biomedical breast model that mimics both dielectric and optical properties of the human breast. The electromagnetic properties of the breast tissue and the tumor are defined as follows. The skin had a conductivity  $\sigma$  of 4 S/m, a relative permittivity  $\epsilon$  of 36 and a thickness of 2 mm. The breast tissue was represented by using a first order Debye model with  $\epsilon_s = 10$ ,  $\epsilon_\infty = 7$ , and  $\sigma = 0.15$  S/m. The tumor is a smaller sphere of diameter of 5 mm. The tumor's electromagnetic properties are given in terms of a Debye model with  $\epsilon_s = 54$ ,  $\epsilon_\infty = 4$ , and  $\sigma = 0.7$  S/m. The tumor was located inside the breast model near the skin tissue. Fig. 5 shows the biomedical breast model used in this study, and Fig. 6 shows the measurement set-up.



FIGURE 5. Photograph of the standard biomedical breast model used in this study. Phantom size: diameter 136 mm and height 70 mm.

The antennas were embedded in the hemispherical resin cup that accommodates the breast model. The dielectric constant of the hemispherical resin cup is 3.6 with a loss tangent of 0.04. Back-lobe radiation from each antenna was suppressed with a metallic housing. Appropriate gap between antenna and the housing was necessary to prevent the antenna's radiation characteristics being affected. Moreover, due to the close contact between the breast and the antenna, a lossy matching fluid was unnecessary to reduce the influence of surrounding structures.

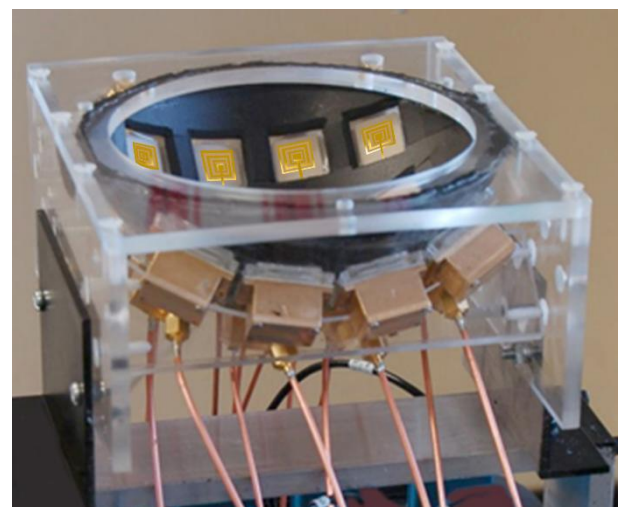


**FIGURE 6.** Prototype set-up of the experimental imaging system.

Measurements were performed using a Vector Network Analyzer (VNA) at fixed spot frequencies, which are within the operating range of the antenna. The noise floor of the system was quantified before imaging the breast model. The noise floor of the setup was around  $-110$  dB with respect to an input power of  $10$  dBm. The magnitude of the tumor response was between  $-45$  dB and  $-80$  dB. The frequency-domain data acquired from the VNA was pre-processed prior to imaging. Firstly, the calibration scan was subtracted from the breast model. Next, the frequency-domain data was converted to the time-domain using inverse Fast Fourier Transform for inverse processing. Tomographic Iterative GPU-based Reconstruction (TIGRE) Toolbox was used to reconstruct the image from the scattered fields in the breast model [54],[55]. TIGRE is an open source toolkit by Engineering Tomography Lab and the European Organization for Nuclear Research (CERN), and it is available for Matlab and Python. Data from the scattered field from the breast model inside the hemispherical cup of radius  $60$  mm were measured at specified radial positions ( $r_1, r_2, \dots, r_N$ ). The reconstruction algorithm used here assumes there are  $M$  scatterers inside the hemispherical cup located at ( $r_{p1}, r_{p1}, \dots, r_{pN}$ ) then the computation of the scattered field vector is defined by

$$\bar{E}_s(f) = \bar{A}(f) \cdot \bar{b}(f) \quad (5)$$

where  $f$  is the frequency,  $\bar{A}$  is the  $[N, M]$  propagator whose  $n$ -th column has the form  $\bar{G}^n = [G^2(r_1, r_n; f), G^2(r_2, r_n; f), \dots, G^2(r_N, r_n; f)]^T$ ,  $\bar{G}$  is the Green's function, and  $\bar{b}$  is the  $[M, 1]$  vector of the inhomogeneities scattering coefficients. The locations of scatterers is computed using

$$P(r_i) = 1/|\log(\langle \bar{G}^i(f_1), \bar{u}_1(f_1) \rangle \cdot \langle \bar{G}^i(f_2), \bar{u}_1(f_2) \rangle)| \quad (6)$$

where  $\bar{G}^i$  is computed at the trial position  $r_i$ , and  $\langle \bar{G}^i(f_1), \bar{u}_1(f_1) \rangle \cdot \langle \bar{G}^i(f_2), \bar{u}_1(f_2) \rangle$  represents the Hermitian scalar product. Detection of tumor is carried out by collecting the scattered field at fixed locations around the breast model. This data in the time-domain is then transformed to frequency domain using Fourier analysis before it can be applied in Eqn. (6).

Initially no tumor was placed in the breast model. Each antenna was excited individually with a microwave pulse of short duration and the backscatter response was collected at the same antenna. This process was repeated for each antenna in the array. The resulting backscatter waveforms stored are of the incident signal and skin backscatter. The image of the breast model with no tumor at two arbitrary spot frequencies are shown in Fig. 7.

A tumor was then inserted in the breast model and the process was repeated. A reference waveform was obtained by averaging the stored waveforms. The skin backscatter and incident signals remain dominant in this reference waveform while the tumor backscatter is reduced to negligible level. The reference waveform was then subtracted from each of the original backscatter waveforms, resulting in calibrated backscatter waveforms that essentially contain only the tumor response. Fig. 8 shows the reconstructed images of the scattered fields from the standard square patch antenna array and the proposed antenna array at  $5.5$  GHz and  $12$  GHz. The microwave pulses are reflected greatly from the region of the breast with a higher relative permittivity than the normal breast and skin tissue, i.e. the relative permittivity of the tumor is  $54$ , skin is  $36$ , and breast tissue is  $10$ . Higher reflection in the image is represented by intense shading that is leaning towards the red region in the color spectrum.

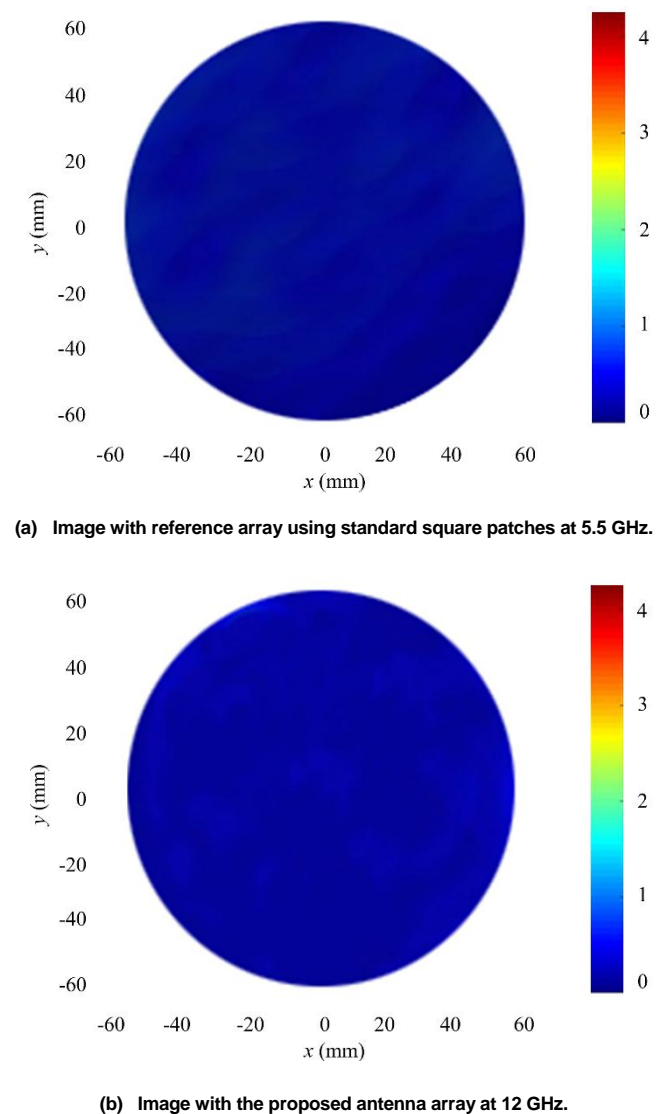
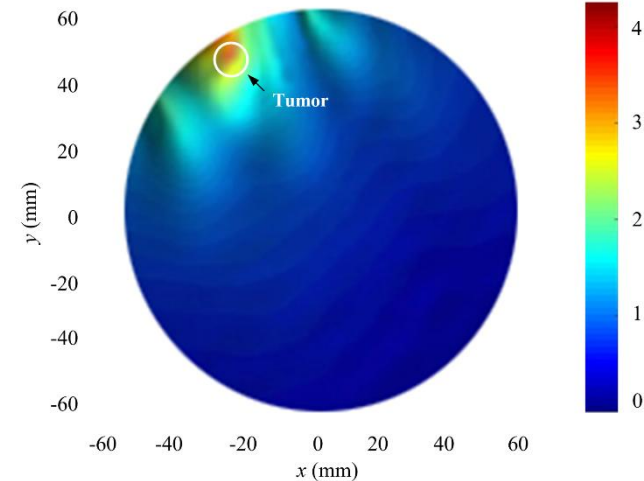
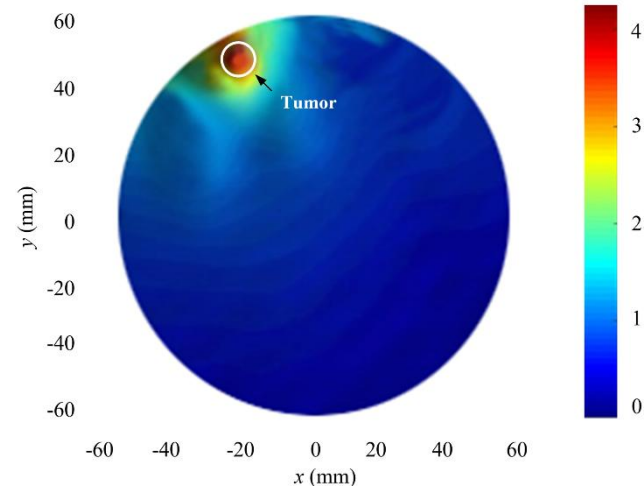


**FIGURE 7.** Image of the breast model with no tumor at (a)  $5.5$  GHz, and (b)  $12$  GHz.

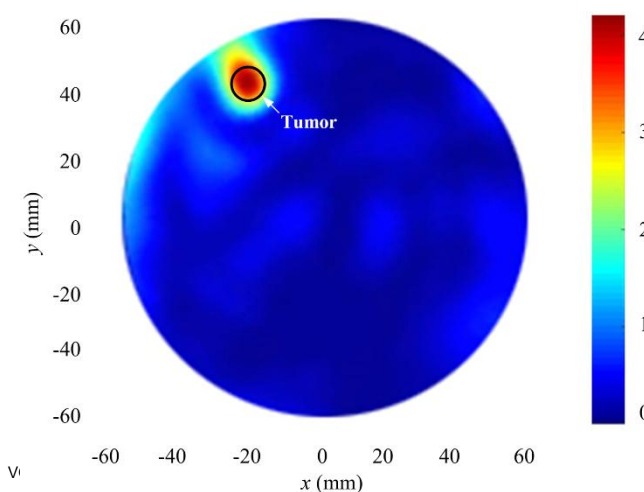
Compared to 5.5 GHz the shorter wavelength at 12 GHz gives better resolution. Close examination of the images from the standard square patch antenna array and the proposed antenna array reveals that with the proposed array provides a better-quality image of the tumor and its location. In fact, the image of the tumor with the proposed antenna array is more distinct and there is reduction in ghosting.



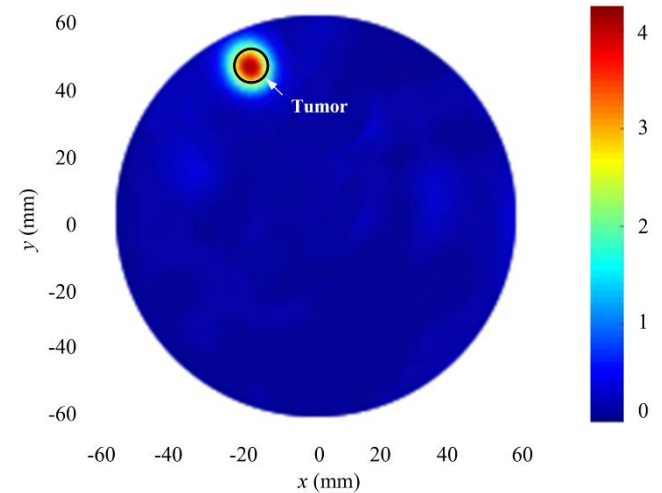
(a) Image with reference array using standard square patches at 5.5 GHz.



(b) Image with the proposed antenna array at 5.5 GHz.



(c) Image with reference array using standard square patches at 12 GHz.



(d) Image with the proposed antenna array at 12 GHz.

**FIGURE 8.** Image of tumor detection using (a) reference antenna array using standard patches at 5.5 GHz, (b) the proposed antenna array at 5.5 GHz, (c) reference antenna array at 12 GHz, and (d) the proposed antenna array at 12 GHz.

## V. CONCLUSION

In this study we have shown that a metamaterial inspired antenna, where the resonant elements have sub-wavelength dimensions, provide superior radiation characteristics than a conventional square patch antenna of identical dimensions. In addition, the proposed antenna is shown to exhibit significantly improved isolation, which is necessary to mitigate unwanted mutual coupling between adjacent radiators that can adversely affect the radiation characteristics of array. This means that an antenna array implemented with the proposed antenna avoids the use of decoupling structures which are normally inserted between radiators. The proposed antenna was used in an array consisting of several radiation elements as biosensors in a microwave imaging system to detect malignant tumors in breasts. The antennas in the array were positioned to surround the biological tissue, i.e. a human breast, under investigation. Each antenna in the array transmitted microwave pulses in turn while all other antennas were used to measure the transmission and reflected signals from abnormalities in the breast. This configuration enables the tumor to be accurately localized. Compared to other antennas reported in literature used in microwave imaging systems the proposed antenna has a small form factor, higher radiation gain (average 11 dBi) and significantly larger impedance bandwidth (2 GHz to 12 GHz) for  $S_{11} \leq -20$  dB making it highly receptive to weak signals. Although proposed antenna array is configured in a hemisphere shape however the array can be adapted to detect tumors in other organs of the human body.

## ACKNOWLEDGMENT

This work is partially supported by RTI2018-095499-B-C31, Funded by Ministerio de Ciencia, Innovación y Universidades, Gobierno de España (MCIU/AEI/FEDER,UE), and innovation programme under grant agreement H2020-MSCA-ITN-2016 SECRET-722424 and the financial support from the UK Engineering and Physical Sciences Research Council (EPSRC) under grant EP/E022936/1.

## REFERENCES

- [1] M. Asefi, A. Baran, and J. LoVetri, "An experimental phantom study for air-based quasi-resonant microwave breast imaging," *IEEE Trans. Microw. Theory Techn.*, Early Access, pp. 1-9, April 2019.
- [2] R. K. Amineh, A. Khalatpour and N. K. Nikolova, "Three-dimensional microwave holographic imaging using co- and cross-polarized data," *IEEE Trans. on Antenna and Propag.*, vol. 60, no. 7, pp. 3526-3531, July 2012.
- [3] M. Asefi, A. Zakaria, and J. LoVetri, "Microwave imaging using normal electric-field components inside metallic resonant chambers," *IEEE Trans. Microw. Theory Techn.*, vol. 65, no. 3, pp. 923-933, Mar. 2017.
- [4] F. Yang et al., "A large-scale clinical trial of radar-based microwave breast imaging for asian women: Phase I," *Proc. IEEE Int. Symp. Antennas Propag.*, USNC/URSI Nat. Radio Sci. Meeting, Jul. 2017, pp. 781-783.
- [5] K. Xu, Y. Zhong, and G. Wang, "A hybrid regularization technique for solving highly nonlinear inverse scattering problems," *IEEE Trans. Microw. Theory Techn.*, vol. 66, no. 1, pp. 11-21, Jan. 2018.
- [6] P. Palmer, G. Hanson, and J. Honeyman-Buck, *Diagnostic imaging in the community, a manual for clinics and small hospitals*: Pan-American Health Organization World Health Organization, 2012.
- [7] S. C. Hagness, A. Taove, and J. E. Bridges, "Three-dimensional FDTD analysis of a pulsed microwave confocal system for breast cancer detection: Design of an antenna-array element," *IEEE Transactions on Ant. and Propag.*, vol. 47, no. 5, pp.783-791, 1999.
- [8] E. C. Fear, and M. A. Stuchl, "Microwave detection of breast cancer," *IEEE Trans. on Microw. Theory & Tech.*, vol. 48, no. 11, pp.1854-1863, 2000.
- [9] D. J. Pagliari, A. Pulimeno, M. Vacca, J. A. Tobon, F. Vipiana, M. R. Casu, and L. P. Carloni, "A low-cost, fast, and accurate microwave imaging system for breast cancer detection," *IEEE Biomedical Circuits and Systems Conference (BioCAS)*, pp.1-4, 2015.
- [10] M. A. Aldhaeabi, T. S. Almoneef, H. Attia, O. M. Ramahi, "Electrically small magnetic probe with PCA for near-field microwave breast tumors detection," *Progress in Electromagnetics Research M*, vol. 84, pp. 177-186, 2019.
- [11] M. A. Aldhaeabi, K. Alzoubi, T. S. Almoneef, S. M. Bamatraf, H. Attia, O. M. Ramahi, "Review of microwaves techniques for breast cancer detection," *Sensors*, vol. 20, 2390, 2020.
- [12] A. J. Surowiec, S. S. Stuchly, J. R. Barr, and A. A. S. A. Swarup, "Dielectric properties of breast carcinoma and the surrounding tissues," *IEEE Trans. on Biomedical Eng.*, vol. 35, no. 4, pp.257-263, 1988.
- [13] T.M Grzegorzczuk, P. M. Meaney, P. A. Kaufman, and K. D. Paulsen, "Fast 3-D tomographic microwave imaging for breast cancer detection," *IEEE Transactions on Medical Imaging*, vol. 31, no. 8, pp.1584-1592, 2012.
- [14] M. Moosazadeh, and S. Kharkovsky, "Design of ultra-wideband antipodal Vivaldi antenna for microwave imaging applications," *IEEE Int. Conf. on Ubiquitous Wireless Broadband*, pp.1-4, 2015.
- [15] G. Ruvio, M. J. Ammann, M. John, R. Solimene, A. D'Alterio, and R. Pierri, "UWB breast cancer detection with numerical phantom and Vivaldi antenna," *IEEE Int. Conf. on Ultra-Wideband*, pp.8-11, 2011.
- [16] M. Molaie, A., M. Kaboli, S. A. Mirtaehri, and M. S. Arshamian, "Dielectric lens balanced antipodal Vivaldi antenna with low cross-polarisation for ultra-wideband applications," *IET Microwaves, Antennas & Propagation*, vol. 8, no. 14, pp.1137-1142, 2014.
- [17] Y. Li, E. Porter, A. Santorelli, M. Popović, M. Coates, "Microwave breast cancer detection via cost-sensitive ensemble classifiers: phantom and patient investigation," *Biomed. Signal Process.*, vol.31, pp. 366-376, 2017.
- [18] M. Naser-Moghadasi, R. A. Sadeghzadeh, T. Aribi, T. Sedghi, and B. S. Virdee, "UWB monopole microstrip antenna using fractal tree unit-cells," *Microwave and Optical Technology Letters*, vol. 54, no. 10, pp. 2366-2370, 2012.
- [19] A. M. Abbosh, H. K. Kan, and M. E. Bialkowski, "Compact ultra-wideband planar tapered slot antenna for use in a microwave imaging system," *Microwave and Optical Technology Letters*, vol. 48, no. 11, pp. 2212-2216, 2006.
- [20] D. Gibbins, M. Klemm, I. J. Craddock, J. A. Leendertz, A. Preece, and R. Benjamin, "A comparison of a wide-slot and a stacked patch antenna for the purpose of breast cancer detection," *IEEE Trans. on Antennas and Propagation*, vol. 58, no. 3, pp.665-674, 2010.
- [21] M. M. Islam, M. T. Islam, M. Samsuzzaman, and M. R. I. Faruque, "A negative index metamaterial antenna for UWB microwave imaging applications," *Microwave and Optical Technology Letters*, vol. 57, no. 6, pp.1352-1361, 2015.
- [22] M. S. S. Alwan, Z. Katbay, "Investigation of tumor using an antenna scanning system," *IEEE Microwave Symp.*, 171, pp.1401-1406, 2014.
- [23] X. Zhao, H. Zhuang, S. C. Yoon, Y. Dong, W. Wang, W. Zhao, "Electrical impedance spectroscopy for quality assessment of meat and fish: A review on basic principles, measurement methods, and recent advances," *J. Food Qual.*, pp.1-16, 2017.
- [24] A. Martellosio, M. Pasian, M. Bozzi, L. Perregrini, A. Mazzanti, F. Svelto, P. E. Summers, G. Renne, L. Preda, M. Bellomi, "Dielectric properties characterization from 0.5 to 50 GHz of breast cancer tissues," *IEEE Trans. Microw. Theory*, vol. 65, pp. 1-14, 2017.
- [25] S. Bharati, P. Rishi, S. K. Tripathi, A. Koul, "Changes in the electrical properties at an early stage of mouse liver carcinogenesis," *Bioelectromagnetics*, vol. 34, pp. 429-436, 2013.
- [26] T. R. Cameron, M. Okoniewski, E. C. Fear, D. Mew, B. Banks, T. A. Ogilvie, "A preliminary study of the electrical properties of healthy and diseased lymph nodes," *Proceedings of the IEEE International Symposium on Antenna Technology and Applied Electromagnetics & the American Electromagnetics Conference*, Ottawa, Canada, pp. 1-3, 2010.
- [27] J. P. Grant, R.N. Clarke, G.T. Symm, N.M. Spyrou, "In vivo dielectric properties of human skin from 50 MHz to 2.0 GHz," *Phys. Med. Biol.*, vol. 33, pp. 607, 1988.
- [28] R. M. Irastorza, E. Blangino, C. M. Carlevaro, F. Vericat, "Modeling of the dielectric properties of trabecular bone samples at microwave frequency," *Med. Biol. Eng. Comput.*, vol. 52, pp. 439-447, 2014.
- [29] L. M. Lue, P.A. Boyden, "Abnormal electrical properties of myocytes from chronically infarcted canine heart alterations in Vmax and the transient outward current," *Circulation*, vol. 85, pp. 1175-1188, 1992.
- [30] J. L. Schepps, K. R. Foster, "The UHF and microwave dielectric properties of normal and tumour tissues: variation in dielectric properties with tissue water content," *Phys. Med. Biol.*, vol. 25, pp. 1149-1159, 1980.
- [31] L. Sha, E. R. Ward, B. Story, "A review of dielectric properties of normal and malignant breast tissue," *Proceedings of the IEEE Southeast Conf.*, Columbia, SC, USA, pp. 457-462, 2002.
- [32] R. Pethig, "Dielectric properties of biological materials: Biophysical and medical applications," *IEEE Trans. Electr. Insul.*, 19, pp. 453-474, 1984.
- [33] M. Lazebnik, M. Okoniewski, J. H. Booske, S. C. Hagness, "Highly accurate Debye models for normal and malignant breast tissue dielectric properties at microwave frequencies," *IEEE Microw. Wirel. Compon.*, vol. 17, pp. 822-824, 2007.
- [34] W. T. Joines, Y. Zhang, C. Li, R. L. Jirtle, "The measured electrical properties of normal and malignant human tissues from 50 to 900 MHz," *Med. Phys.*, vol. 21, pp.547, 1994.
- [35] M. Lazebnik, D. Popovic, L. McCartney, C. Watkins, M. Lindstrom, J. Harter, S. Sewall, T. Ogilvie, A. Magliocco, T. M. Breslin, et al., "A large-scale study of the ultrawideband microwave dielectric properties of normal, benign and malignant breast tissues obtained from cancer surgeries," *Phys. Med. Biol.*, vol.52, pp. 2637-2656, 2017.

- [36] S. S. Chaudhary, R. K. Mishra, A. Swarup, J.M. Thomas, "Dielectric properties of normal & malignant human breast tissues at radiowave & microwave frequencies," *Indian J. Biochem. Biol.*, vol.21, pp. 76–79, 1984.
- [37] A. Swarup, S. S. Stuchly, A. Surowiec, "Dielectric properties of mouse MCA1 fibrosarcoma at different stages of development," *Bioelectromagnetics*, vol.12, pp.1, 1991.
- [38] A. J. Surowiec, S. S. Stuchly, J. R. Barr, A. Swarup, "Dielectric properties of breast carcinoma and the surrounding tissues," *IEEE Trans. Biomed. Eng.*, vol.35, pp. 257–263, 1988.
- [39] T. Said, V. V. Varadan, "Variation of Cole-Cole model parameters with the complex permittivity of biological tissues," *IEEE MTT-S International Microwave Symposium Digest (MTT'09)*, Boston, MA, USA, pp. 1445–1448, 2009.
- [40] S. Mustafa, A.M. Abbosh, P.T. Nguyen, "Modeling human head tissues using fourth-order Debye model in convolution-based three-dimensional finite-difference time-domain," *IEEE Trans. Antenna Propag.*, vol.62, pp. 1354–1361, 2014.
- [41] K. Kang, X. Chu, R. Dilmaghani, M. Ghavami, "Low-complexity Cole-Cole expression for modelling human biological tissues in (FD)2TD method," *Electron. Lett.*, vol.43, pp. 143–144, 2017.
- [42] M. Alibakhshikenari, B. S. Virdee, P. Shukla, C. H. See, R. Abd-Alhameed, M. Khalily, F. Falcone, E. Limiti, "Interaction between closely packed array antenna elements using meta-surface for applications such as MIMO systems and synthetic aperture radars," *Radio Science*, vol.53, Issue 11, pp. 1-15, 2018.
- [43] C. Carlos and T. Itoh, *Electromagnetic Metamaterials: Transmission Line Theory and Microwave Applications*, John Wiley & Sons, New York, USA, 2005.
- [44] M. M. Nikolic', A. R. Djordjevic', and A. Nehorai, "Microstrip antennas with suppressed radiation in horizontal directions and reduced coupling," *IEEE Transactions on Antennas and Propagation*, vol. 53, no. 11, pp. 3469-3476, 2005.
- [45] J. Ghosh, D. Mitra, S. Das, "Mutual coupling reduction of slot antenna array by controlling surface wave propagation," *IEEE Transactions on Antennas and Propagation*, vol.67, no. 2, pp. 1352-1357, 2019.
- [46] S. Xu, M. Zhang, H. Wen, and J. Wang, "Deep-subwavelength decoupling for MIMO antennas in mobile handsets with singular medium," *Scientific Reports*, 7: 12162, pp.1-9, 2017.
- [47] H. Luan, C. Chen, W. Chen, L. Zhou, H. Zhang, and Z. Zhang, "Mutual coupling reduction of closely E/H-plane coupled antennas through metasurfaces," *IEEE Antennas and Wireless Propagation Letters*, vol.18, no. 10, pp.1996-2000, 2019.
- [48] A. Jafargholi, A. Jafargholi, J. H. Choi, "Mutual coupling reduction in an array of patch antennas using CLL metamaterial superstrate for MIMO applications," *IEEE Transactions on Antennas and Propagation*, vol.67, no. 1, pp.179-189, 2019.
- [49] M. Z. Mahmud, et al., "Microwave imaging for breast tumor detection using uniplanar AMC based CPW-fed microstrip antenna," *IEEE Access*, vol.6, pp. 44763-44775, 2018.
- [50] A. Aziz, et al., "On-body circular patch antenna for breast cancer," *IEEE Int. Electromagnetics and Antenna Conf.*, pp. 029-034, 2019.
- [51] R. Karli, et al., "Miniature planar ultra-wide-band microstrip antenna for breast cancer detection," *16<sup>th</sup> Mediterranean Microw. Symp.*, pp. 1-4, 2016.
- [52] M. A. Aldhaeb, T. S. Almoneef, H. Attia, and O. M. Ramahi, "Near-field microwave loop array sensor for breast tumor detection," *IEEE Sensors Journal*, vol.19, no14, pp. 1187-11872, 2019.
- [53] M. Rokunuzzaman, M. Samsuzzaman, M. T. Islam, "Unidirectional wideband 3-D antenna for human head-imaging application," *IEEE Ant. and Wireless Propagation Letters*, vol. 16, pp. 169–172, 2017.
- [54] A. Biguri, M. Dosanjh, A. Hancock, and M. Soleimani, "TIGRE: A MATLAB-GPU Toolbox for CBCT Image Reconstruction," *Biomedical Physics & Eng. Express*, vol. 2, no. 5, 055010, 2016.
- [55] S. Kazemi, O. Diaz, P. Elangovan, K. Wells, and A. Lohstroh, "Validation and application of a new image reconstruction software toolbox (TIGRE) for breast cone-beam computed tomography," *Medical Imaging: Physics of Medical Imaging*, Proc. SPIE, 2018.